RSC Advances

PAPER

View Article Online
View Journal | View Issue

Cite this: *RSC Adv.*, 2020, **10**, 26521

Novel cross-linked poly(vinyl alcohol)-based electrolyte membranes for fuel cell applications

Poonkuzhali Kulasekaran, Berlina Maria Mahimai and Paradesi Deivanayagam *

Herein, a new series of polymer electrolyte membranes was prepared by chemically cross-linked poly(vinyl alcohol) (PVA) and sulfonated poly(ether sulfone) (SPES). A typical polymerization reaction was conducted using three different monomers *i.e.* bisphenol A, phenolphthalein, and 4,4′-dichlorodiphenyl sulfone. The SPES polymer was obtained by the post-sulfonation technique using chlorosulfonic acid as a sulfonating agent. The resultant SPES polymer at different concentrations was blended with cross-linked poly(vinyl alcohol). Structural analysis of the samples was conducted by FTIR, SEM, and XRD. Among the prepared PEM materials, PVA–SPES-20 blend membranes exhibited higher ion-exchange capacity and % water uptake values than those of the other membranes. In addition, the PVA–SPES-20 membrane exhibits the proton conductivity of 0.0367 S cm^{-1} at 30 °C, whereas pristine PVA shows the proton conductivity of 0.0259 S cm^{-1}. The overall experimental results revealed that the PVA–SPES blend membranes are promising candidates for fuel cell applications.

Received 15th May 2020
Accepted 25th June 2020

DOI: 10.1039/d0ra04360e

rsc.li/rsc-advances

Introduction

With the increasing growth of human population and activities, energy consumption has increased. Fuel cells are an alternative energy source because of their high efficiency.[1,2] A fuel cell is an electrochemical device that converts chemical energy into electrical energy with almost zero emission of pollutants.[3,4] Among the various types of fuel cells, polymer electrolyte membrane fuel cells (PEMFCs) are the most desirable power sources because of their high efficiency, simple system features, and wide applications in transportation, aerospace, and mobile power stations.[5,6] Proton exchange membranes (PEMs) are a key component and play major role in the transport of protons from the anode to the cathode in PEMFCs.[7] The most commonly used polyelectrolytes in PEMFCs are perfluorosulfonic acid membranes, such as Nafion, due to their durability and flexibility.[8,9] Nafion exhibits excellent proton conductivity, higher water uptake, and good thermal and mechanical properties.[10] However, it has many drawbacks such as complicated synthetic procedure, loss of ionic conductivity at higher temperatures, and high cost, which hinder its further applications.[11,12] This is the reason that the current research focuses on the development of alternative proton conducting membranes comparable to Nafion in terms of technical and economic viability for fuel cell applications.[13]

Poly(vinyl alcohol)-based electrolyte membranes are most desirable candidates due to their extensive applications in fuel cells.[14–16] PVA is one of the cost-effective synthetic semi-crystalline polymers, which has significant properties such as good film forming ability, excellent thermal and mechanical stability, and favourable chemical cross-linking ability.[17–19] PVA-based membranes possess excellent water uptake capacity, high strength and flexibility, and low methanol permeability. However, due to the absence of charge functional groups, such as sulfonic acid ($-SO_3H$)/carboxylic acid (–COOH) groups, the PVA membranes exhibit low ionic conductivity.[20] Strong ionic groups, such as sulfonic groups, phosphonic groups, and quaternary ammonium salts, are commonly used proton sources in polymeric membranes. The incorporation of proton sources into the PVA matrix is a better option to improve the ionic conductivity and hydrophilicity of PVA membranes.[21] In general, the amount of sulfonic acid groups present in the membrane facilitates more proton conductivity. The incorporation of grafted sulfonic acid moieties improves the electrochemical properties of membranes because the sulfonic acid groups reduce the effect of main chain and increase the water volume fraction by the ion-cluster effect. However, they cause some drawbacks such as high fuel crossover, loss of conductivity at elevated temperatures, and slow cathode kinetics.[22]

Modification of the PVA matrix will help to enhance the conductivity of PVA membranes. According to previous studies, PVA membranes have been modified through three different methods: (i) grafting copolymerization,[23] (ii) physical and chemical cross-linking,[24] and (iii) blending of polymers.[25] These types of modifications will improve the physicochemical properties of PVA membranes and thereby lead to their significant application in fuel cells. In recent years, many researchers have become interested in the preparation of non-fluorinated

Department of Chemistry, Faculty of Engineering and Technology, SRM Institute of Science and Technology, Kattankulathur, Tamil Nadu, India. E-mail: paradesi77@yahoo.com

aromatic hydrocarbon-based PEMs such as sulfonated poly phthalazinone (SPP),[26,27] polybenzimidazole (PBI),[28,29] sulfonated poly(ether sulfone) (SPES),[30,31] and sulfonated poly(ether ether ketone) (SPEEK).[32,33]

Poly ether sulfone (PES) is one of the aromatic hydrocarbons that belong to the poly(arylene ether sulfone) family. In general, the PES polymer shows good thermal and mechanical stability, ease of modification, water retention capacity, ion-exchange ability, *etc.*[34] *Via* sulfonation, the water uptake ability and ionic conductivity of the PES polymer can be increased.[35] Sulfonated polymer electrolytes can be obtained by either the sulfonation of a base polymer[36,37] or the synthesis of a polymer using a pre-sulfonated monomer.[38,39] PVA-based electrolyte membranes exhibit good mechanical and chemical stabilities, which are adequate for their use in the preparation of polymer electrolyte membranes. PVA itself does not exhibit ionic conductivity; however, the introduction of several organic groups, such as carboxylates, sulfonates, amines, and quaternary ammonium, produces more hydrophilic characteristics and thereby enhances the proton conductivity of PVA.[40,41] Hence, polymers, such as SPES, containing sulfonic acid groups have been chosen to combine with PVA to alleviate the proton conductivity of PVA membranes.

In this study, a new series of polymer blend membranes based on cross-linked PVA and SPES was designed, and the properties of these membranes were studied in detail. The PVA matrix was cross-linked using glutaraldehyde as a cross-linking agent. The –OH groups of PVA react with the –CHO group of the crosslinker to form acetal or hemiacetal linkages, and the cross-linked PVA has a gel-like nature. Furthermore, it is water insoluble and has the ability to form a large thin membrane. This cross-linked PVA was blended with the SPES polymer at different weight percentages. These types of electrolyte membranes are suitable materials for the enhancement of fuel cell performance.

Experimental

Materials

Poly(vinyl alcohol), 4,4′-dichlorodiphenyl sulfone (DCDPS), and phenolphthalein were purchased from Sigma-Aldrich Co., USA. Bisphenol A, anhydrous potassium carbonate, *N*-methyl-2-pyrrolidone (NMP), dimethyl sulfoxide (DMSO), glutaraldehyde (GA), and sulfuric acid were procured from Sisco Research Laboratories Pvt. Ltd., Mumbai, India.

Synthesis of sulfonated poly(ether sulfone)

Typical polymerization was carried out using three different monomers, namely bisphenol A (10 mmol, 2.28 g), phenolphthalein (10 mmol, 3.18 g), and 4,4′-dichlorodiphenyl sulfone (20 mmol, 5.76 g), in a 250 mL round-bottom flask equipped with a magnetic stirrer, Dean–Stark trap, and nitrogen inlet. The schematic of the synthesis of the SPES polymer is shown in Scheme 1. Initially, all the monomers were completely dissolved using a solvent, NMP (20 mL) under constant stirring. Then, 10 mL toluene and anhydrous potassium carbonate (40 mmol, 5.52 g) were added to the abovementioned solution followed by refluxing at 150 °C for 5 h. After the controlled removal of toluene by distillation, the reaction mixture was continuously stirred at 180 °C for 18 h. The resultant viscous polymer solution was slowly cooled to room temperature followed by dilution with NMP for easy filtration. The filtered solution was slowly transferred to a beaker containing excess methanol. The precipitated PES polymer was washed several times with ethanol and dried at 100 °C under vacuum for 12 h. Sulfonation of the prepared PES polymer was carried out using chlorosulfonic acid as a sulfonating agent and dichloroethane as a solvent under constant stirring at 0–5 °C for 2 h. After the evaporation of the solvent, the SPES polymer was obtained as a precipitate and washed several times with water till the pH of the washed water became neutral.

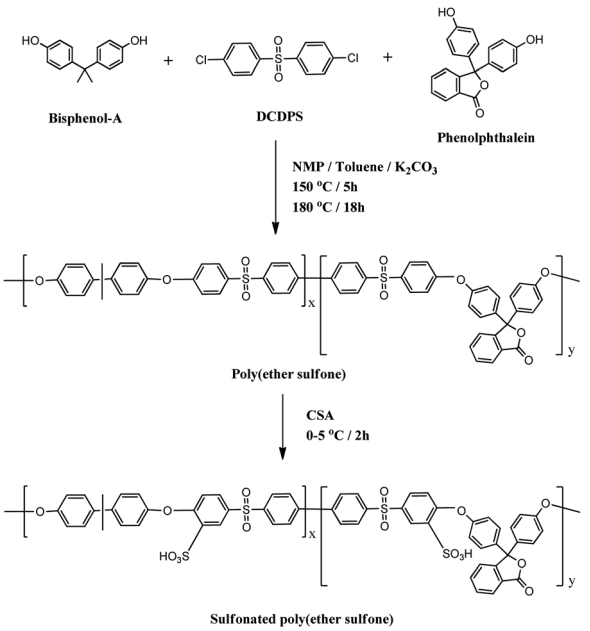

Scheme 1 Schematic for the synthesis of sulfonated poly(ether sulfone).

Preparation of PVA/SPES blend membranes

At first, PVA in appropriate quantity was dissolved in DMSO under constant stirring. Then, the SPES polymer in a desired amount (5–20 wt%) was added to the PVA polymer solution under constant stirring at 60 °C. The temperature of the reaction mixture was slowly increased to 80 °C and maintained for 6 h. A cross-linking agent, GA (1 mL), was gradually added through a micropipette to the PVA solution at 40 °C followed by stirring for 30 min. Subsequently, 2 M H_2SO_4 (0.5 mL) as a catalyst was added for the cross-linking reaction. The resultant viscous solution was cast on a flat glass plate and kept in a closed chamber for 24 h. After this, the membrane in the glass plate was dried in a hot air oven at 60 °C for 6 h. The prepared PVA/SPES membranes were thoroughly washed with plenty of deionized water and again dried at 100 °C for 12 h under

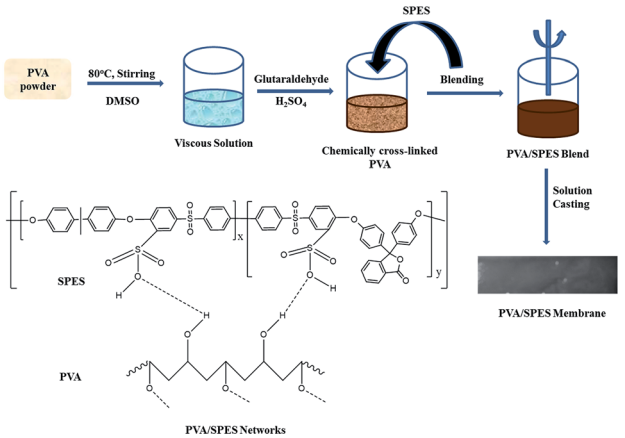

Scheme 2 Schematic for the preparation of the PVA/SPES blend membranes.

vacuum. The schematic of the steps conducted to obtain the PVA/SPES blend membranes is depicted in Scheme 2.

Measurements

FTIR spectra of the polymers were recorded using a MIRacle 10, Single Reflection HATR, Shimadzu IRTracer-100 spectrometer (Japan). Infrared spectra were obtained in the absorption mode with 32 scans at a resolution of ±4 cm^{-1} covering the wavenumber range of 4000–400 cm^{-1}. X-ray diffraction analysis was conducted by an X'Pert diffractometer with Cu-Kα radiation ($\lambda = 1.5405$ Å) operating at 40 kV and 30 mA in the 2θ range of 5–90°. XRD patterns were acquired at a scan rate of 0.5° min^{-1}. The morphology study was carried out by an electron microscope that produces images of a sample by scanning the surface with a focused beam of electrons. The SEM images of the electrolyte membranes were obtained using a field-emission scanning electron microscope (FEI, Quanta FEG 200, Hillsboro, OR, USA).

The IEC of the prepared polyelectrolyte membranes was calculated by the back-titration method using phenolphthalein as an indicator. At first, the dried membrane was acidified with a 0.10 M HCl solution. Subsequently, it was properly dried and then soaked in 50 mL of a 1.0 M NaCl solution for 24 h. As a result, all the H^+ ions migrated into the solution by ion-exchange reactions with Na^+ ions. The resultant solution was titrated against a 0.01 M NaOH solution. From the titre value, the IEC of the membrane was calculated using eqn (1):

$$\text{IEC (meq. g}^{-1}) = (V \times N)/\text{weight of the polymer} \quad (1)$$

where V is the volume of the NaOH solution consumed and N is the normality of the NaOH solution.

Water uptake ability and swelling ratio of the electrolyte membranes were measured as per the procedure reported in our previous study.[42] Thermogravimetric analysis (TGA) was used to investigate the thermal stability of the polymers. Samples were heated from room temperature to 600 °C at the rate of 10 °C min^{-1} under a N_2 atmosphere. Oxidative stability of the prepared PEMs was analysed by immersing the membrane sample in 50 mL Fenton's reagent at room temperature for 5 h. The membrane sample was withdrawn from the Fenton's reagent and weighed again to evaluate the weight loss percentage.

As a measure of the hydrophobicity/hydrophilicity of membrane surface, water contact angle was determined by the sessile drop method using a Holmarc contact angle meter (Model: HO-IAD-CAM-01). The resistance of the electrolyte membrane provides the conductivity (σ) of the membrane. The relationship between the conductivity and resistance is presented by eqn (2).

$$\sigma\ (\text{S cm}^{-1}) = L/RA \quad (2)$$

where L is the thickness of the membrane and A is the area of the membrane under investigation.

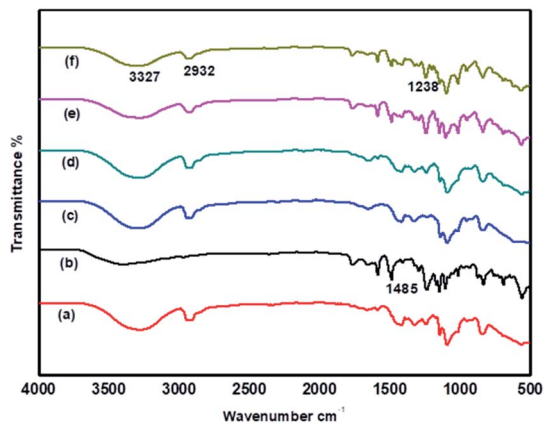

Fig. 1 FTIR spectra of (a) PVA, (b) SPES, and (c) PVA–SPES-5, (d) PVA–SPES-10, (e) PVA–SPES-15, and (f) PVA–SPES-20 membranes.

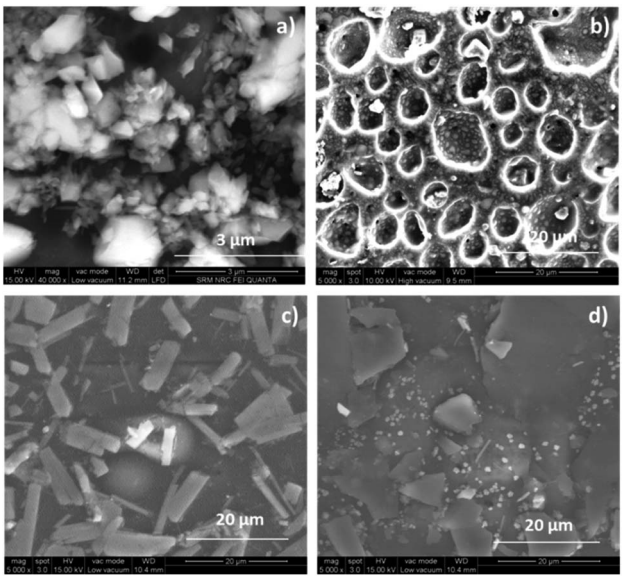

Fig. 2 SEM images of (a) PVA, (b) SPES, and (c) PVA/SPES-10 and (d) PVA/SPES-15 blend membranes.

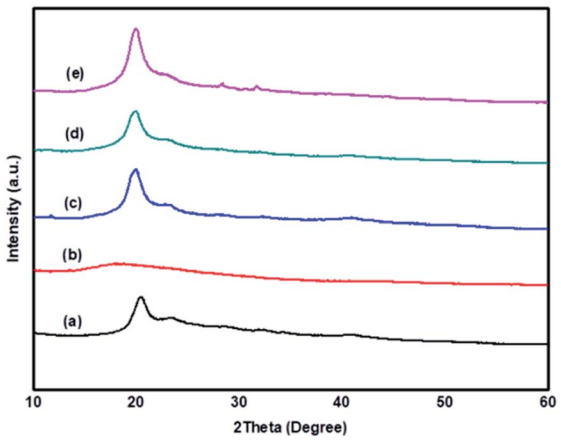

Fig. 3 XRD patterns of (a) PVA, (b) SPES, and (c) PVA–SPES-5, (d) PVA–SPES-10, and (e) PVA–SPES-15 blend membranes.

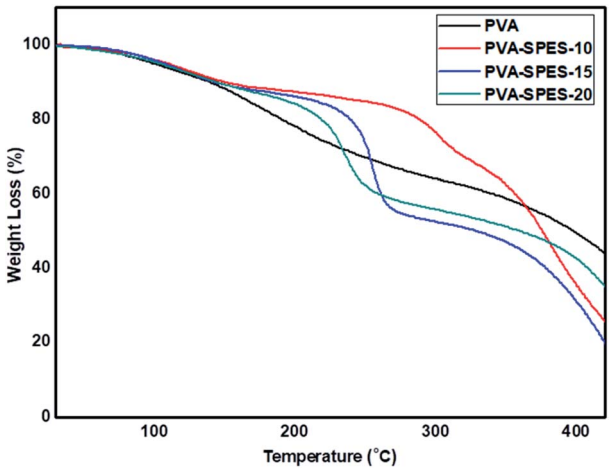

Fig. 4 Thermograms of the PVA and PVA–SPES blend membranes.

Results and discussion

Spectral studies

The functional groups present in the polymer electrolyte membranes were identified by Fourier transform infrared spectroscopy. The FTIR spectra of PVA and PVA/SPES blend membranes are presented in Fig. 1. The broad peak located at 3327 cm^{-1} corresponds to the stretching vibration of the hydroxyl group. The intense signal detected at 1485 cm^{-1} was attributed to the aromatic ring skeleton. The peak around 2932 cm^{-1} corresponds to the C–H stretching frequency of the alkyl group. The peak at 1148 cm^{-1} was attributed to the symmetric stretching vibration of the sulfone (O═S═O) group. The signal centered at 1238 cm^{-1} confirms the presence of an ether linkage in the polymer chain.

Morphology

Surface morphology of the polymers and blend membranes was investigated by field-emission scanning electron microscopy. Fig. 2 shows the SEM images of PVA, SPES, and blend membranes. The SPES polymer has small pores distributed on its surface. Hence, these pores can retain water molecules and thereby provide good pathway for ion conduction. The morphology of the blend membranes clearly shows the dispersion of ionic domains from the SPES polymer that enhances the proton conductivity of the membranes. Phase separation between the hydrophobic and hydrophilic regions of the membranes is attributed to the enhanced proton conductivity and morphological stability.

XRD analysis

X-ray diffraction is an appropriate method to analyze the structural changes with respect to the crystallinity of the polymer matrix. Fig. 3 shows the XRD patterns of PVA, SPES, and blend membranes. The broad peak observed at $2\theta = 20°$ in the XRD pattern of PVA indicates that PVA has a dual amorphous–crystalline nature.[43] The SPES polymer exhibits a good amorphous nature because of the presence of the hydrophilic sulfonic acid group. The XRD results indicate that although the SPES polymer exhibits amorphous nature, the concentration of PVA is maximum in the polymer blends as compared to that of the SPES polymer; this favours a higher degree of crystallinity and less amorphous behaviour.

Water uptake

It is necessary to measure the amount of water molecules present in the proton-exchange membrane responsible for the transport of protons in the medium. In general, higher water uptake ability of the membrane causes more swelling, which decreases the mechanical strength of the membrane; however, a lack of water molecules reduces the conductivity of the membrane. Both the conductivity and strength of the PEM material influence the performance of fuel cells. Table 1 presents the values of water uptake and swelling ratio for PVA and

Table 1 Physicochemical properties of the PVA and PVA/SPES blend membranes

Polymer code	Composition (g)		Thickness (μm)	IEC (meq. g^{-1})	Water uptake (%)	Swelling ratio (%)
	PVA	SPES				
PVA	1.00	0	24	0.25	50.73	18
PVA–SPES-5	0.95	0.05	26	0.58	51.96	15
PVA–SPES-10	0.90	0.10	25	0.60	55.39	17
PVA–SPES-15	0.85	0.15	26	0.91	61.45	18
PVA–SPES-20	0.80	0.20	25	1.02	77.21	20

blend membranes. The electrolyte membrane blended with 20 wt% SPES retains the maximum water uptake capacity of 77.21%, whereas the pristine membrane exhibits the water uptake capacity of only 50.73%. This result proves that the water uptake capacity of the PVA/SPES blend membrane increases with the increasing concentration of SPES. The hydrophilic nature of the sulfonic acid moiety of SPES helps to alleviate the water uptake capacity of the blend membranes.

IEC and swelling ratio

The number of ionisable functional groups present in the membrane was determined by the back-titration method, and the results are provided in Table 1. The pristine PVA polymer shows an ion-exchange capacity of 0.25 meq. g^{-1} before blending with SPES. The IEC values of the blend membranes are in good agreement with the water uptake values because the loading of SPES onto the PVA matrix leads to higher IEC. The enhancement in the IEC values of the blend membranes is owing to the presence of sulfonic acid groups in the polymer structure. A moderate swelling behaviour (15–20%) was observed for the PVA/SPES blend membranes, which does not affect their thermal stability.

Thermal stability

The thermal stability of the control and blend membranes was investigated by thermogravimetric analysis, and the thermograms are displayed in Fig. 4. All the membranes demonstrated three-step weight losses. The initial weight loss observed at approximately 100 °C was due to the evaporation of the absorbed water molecules. The second weight losses at 235 °C and 216 °C were attributed to the desulfonation of the PVA–SPES-15 and PVA–SPES-20 membranes, respectively. Due to the higher concentration of SPES in the PVA–SPES-20 membrane, more flexibility and thereby more weight loss were observed for the PVA–SPES-20 membrane than those for the PVA–SPES-15 membrane. Final step degradation was observed due to the destruction of the polymer backbone. The TGA results indicated that the prepared PEM materials exhibit sufficient thermal stability for fuel cell operation.

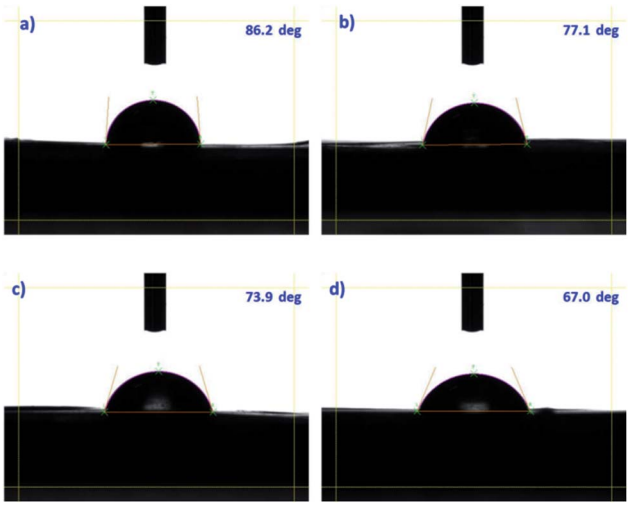

Fig. 6 Contact angle measurement of (a) PVA, (b) SPES, (c) PVA–SPES-15, and (d) PVA–SPES-20.

Oxidative stability

Fenton's test was conducted in order to evaluate the oxidative stability of the prepared electrolyte materials. Fig. 5 displays the retained weight percentage of PVA and blend membranes. The oxidative stability of the PVA membrane was found to be 98.5%, and it slightly decreased when this membrane was incorporated with the SPES polymer. The PVA–SPES-20 membrane retained a weight of 91.6%. These results indicated that free radicals have a slight impact on the oxidative stability of the blend membranes due to the greater oxidative resistivity of these membranes against Fenton's reagent.

Contact angle

Contact angle is a measure of the hydrophilicity/hydrophobicity of the polymer membrane surface. Fig. 6 shows the contact

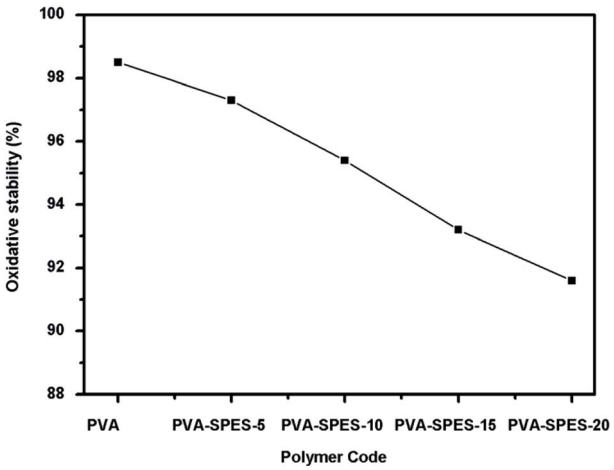

Fig. 5 Oxidative stability of the PVA and PVA–SPES blend membranes.

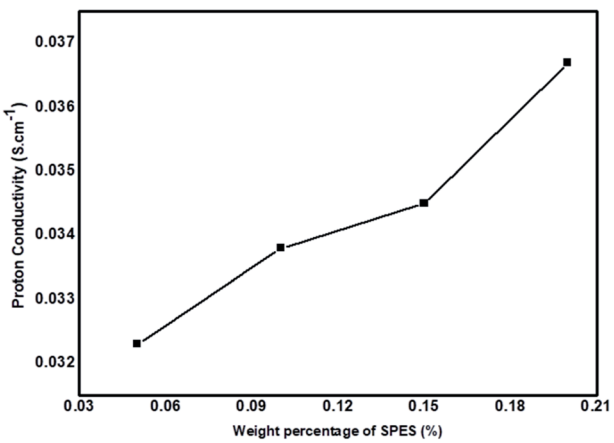

Fig. 7 Influence of the concentration of SPES in the blend membranes on proton conductivity.

Table 2 Comparison between the proton conductivities of various PVA-based electrolyte membranes

S. no.	Polymer electrolyte	Additives	Proton conductivity (S cm^{-1})
1.	PVA/PBI[48]	Polybenzimidazole	0.0027
2.	PVA/STA[49]	Silicotungstic acid	0.0046
3.	GO impregnated PVA–STA[49]	Graphene oxide and silicotungstic acid	0.0720
4.	PVA/Nafion[50]	Nafion and hydroxyapatite	0.0012
5.	PVA–SSA – 0.1 wt% SCNT[51]	Sulfonated carbon nanotube	0.0390
6.	Cross-linked PVA/TiO_2 (ref. 52)	Titanium dioxide	0.0160
7.	CS/PVA/SWA[53]	Chitosan and silicotungstic acid	0.0160
8.	PVA–SPES (present work)	Sulfonated poly(ether sulfone)	0.0367

angle images of the pristine PVA and blend membranes. Both the pristine PVA and PVA/SPES blend membranes possess a contact angle of less than 90°, which clearly proves the hydrophilic nature of the membrane surface due to the presence of polar groups.

Proton conductivity

Proton conductivity is an essential characteristic that enhances the performance and efficiency of fuel cells. However, the proton conductivity of an electrolyte membrane is influenced by many factors such as ion-exchange capacity, water uptake, and amount of sulfonic acid present in the polymer backbone. There are two types of proton transfer mechanisms involved in PEMs: (i) Grotthuss mechanism in which proton transfer occurs between one proton-conducting site to the next, and this is also known as proton-hopping mechanism[44,45] and (ii) vehicle mechanism in which proton transfer occurs through the diffusion of free water molecules.[46,47] The nature of hydrogen bonding between the protonated species and their environment decides the proton conduction mechanism. The strong and weak hydrogen bonding existing in the polymer tends to follow the Grotthuss and vehicle mechanism, respectively.[48] Hence, the PVA/SPES blend membranes follow the vehicle proton transport mechanism.

The influence of the concentration of SPES in the blend membranes on proton conductivity is presented in Fig. 7. The PVA membrane exhibited a proton conductivity of 0.0259 S cm^{-1}, whereas the PVA/SPES blend membranes displayed proton conductivity in the range from 0.0322 to 0.0367 S cm^{-1}. The reason for the improvement in the proton conductivity of the PVA/SPES blend membrane is the increased concentration of the sulfonic acid moiety, which provides a porous texture and thereby aid in the retention of more water. Thus, controlled water uptake ability leads to moderate swelling characteristics and offers a continuous space for proton transport through the membrane. Table 2 presents a comparison between the proton conductivities of PVA–SPES blend membranes and the reported PVA-based electrolyte membranes. The comparison clearly shows that the introduction of heteropoly acids, graphene oxide, functionalized carbon nanotubes, sulfonated polymers, *etc.* into the PVA matrix leads to an enhancement in the proton conductivity.

Conclusion

Herein, a series of polymer blends based on cross-linked PVA and SPES were prepared. The morphology studies confirm the successful incorporation of SPES into the polymer matrix. The water uptake capacity of the polymer membrane was increased with respect to the loading of the SPES polymer and thereby improved the ionic conductivity. The PVA–SPES-20 membrane exhibits the maximum water uptake capacity of 77.21%, whereas the pristine membrane retains the water uptake capacity of 50.73%. The ion-exchange capacity of the blend membrane was increased due to the impregnation of SPES into the PVA matrix. The ionic conductivity of 0.0367 S cm^{-1} was acquired by loading SPES at a concentration of 20 wt% into the PVA matrix. The water retention ability combined with the high ionic conductivity of the PVA/SPES blend membranes make these membranes a viable material for fuel-cell applications.

Conflicts of interest

There are no conflicts to declare.

Acknowledgements

Authors would like to acknowledge DST-FIST (Fund for improvement of S&T infrastructure) for providing financial assistance at Department of Chemistry, SRM Institute of Science and Technology, No. SR/FST/CST-266/2015(c). One of the authors (DP) would like to acknowledge SRM IST for providing financial support under SRM Selective Excellence Scheme.

Notes and references

1 A. B. Stambouli and E. Traversa, *Renewable Sustainable Energy Rev.*, 2002, **6**, 433.
2 A. K. Shukla, R. K. Raman and K. Scott, *Fuel Cells*, 2005, **5**, 436.
3 H. Beydaghi, M. Javanbakht and A. Badiei, *J. Nanostruct. Chem.*, 2014, **4**, 1.
4 V. K. Shahi, *Solid State Ionics*, 2007, **117**, 3395.
5 L. Van Biert, M. Godjevac, K. Visser and P. V. Aravind, *J. Power Sources*, 2016, **327**, 345.

6 H. Ahmad, S. K. Kamarudin, U. A. Hasran and W. R. W. Daud, *Int. J. Hydrogen Energy*, 2011, **36**, 14668.
7 P. Jannasch, *Curr. Opin. Colloid Interface Sci.*, 2003, **8**, 96.
8 J. Ahn, H. Lee, T. H. Yang, C. S. Kim and B. Bae, *J. Polym. Sci.*, 2014, **52**, 2947.
9 E. Erdal Unveren, T. Erdogan, S. S. Celebi and T. Y. Inan, *Int. J. Hydrogen Energy*, 2010, **35**, 3736.
10 H. Wang, B. A. Holmberg, L. Huang, Z. Wang, A. Mitra and J. M. Norbeck, *J. Mater. Chem.*, 2002, **12**, 834.
11 M. Kumari, H. S. Sodaye and R. C. Bindal, *J. Power Sources*, 2018, **398**, 137.
12 D. Paradesi and R. A. Ramanujam, *J. Macromol. Sci., Part A: Pure Appl. Chem.*, 2012, **49**, 191.
13 S. J. Peighambardoust, S. Rowshanzamir and M. Amjadi, *Int. J. Hydrogen Energy*, 2010, **35**, 9349.
14 T. Zhou, Y. Li, W. Wang, L. He, L. Cai and C. Zeng, *Int. J. Electrochem. Sci.*, 2019, **14**, 8514.
15 P. Y. Hsu, T. Y. Hu, S. Rajesh Kumar, C. H. Chang, K. C. W. Wu and K. L. Tang, *Polymers*, 2018, **10**, 102.
16 A. Anis, A. K. Banthia and S. Bandyopadhyay, *J. Mater. Eng. Perform.*, 2008, **17**, 772.
17 H. K. Gopi, V. M. Dhavale and S. D. Bhat, *Mater. Sci. Energy Technol.*, 2019, **2**, 194.
18 S. B. Aziz, O. G. Abdullah, S. A. Hussein and H. M. Ahmed, *Polymers*, 2017, **9**, 622.
19 H. Beydaghi, M. Javanbakht, A. Bagheri, P. Salarizadeh, H. G. Zahmatkesh and S. Kashefi, *RSC Adv.*, 2015, **5**, 74054.
20 S. Shabanpanah, A. Omrani and M. M. Lakouraj, *Des. Monomers Polym.*, 2019, **22**, 130.
21 C. C. Yang, *Int. J. Hydrogen Energy*, 2011, **36**, 4419.
22 Y. Chang, A. D. Mohanty, S. B. Smedley, K. Abu-Hakmeh, Y. H. Lee, J. E. Morgan, M. A. Hickner, S. S. Jang, C. Y. Ryu and C. S. Bae, *Macromolecules*, 2015, **48**, 7117.
23 S. Aoshima, M. Ikeda, K. Nakayama, E. Kobayashi, H. Ohgi and T. Sato, *Polym. J.*, 2001, **33**, 610.
24 K. C. S. Figueiredo, T. L. M. Alves and C. P. Borges, *J. Appl. Polym. Sci.*, 2009, **111**, 3074.
25 T. Yang, *Int. J. Hydrogen Energy*, 2008, **33**, 6772.
26 Y. M. Sun, T. C. Wu, H. C. Lee, G. B. Jung, M. D. Guiver and Y. Gao, *J. Membr. Sci.*, 2005, **265**, 108.
27 F. Ding, S. Wang, M. Xiao and Y. Meng, *J. Power Sources*, 2007, **164**, 488.
28 A. Shabanikia, M. Javanbakht, H. S. Amoli, K. Hooshyari and M. Enhessari, *Electrochim. Acta*, 2015, **154**, 370.
29 P. Staiti, F. Lufrano, A. S. Arico, E. Passalacqua and V. Antonucci, *J. Membr. Sci.*, 2001, **188**, 71.
30 D. Paradesi, R. A. Ramanujam and S. N. Jaisankar, *Polym. J.*, 2013, **45**, 166.
31 N. N. Krishnan, H. J. Kim, M. Prasanna, E. Cho, E. M. Shin, S. Y. Lee, I. H. Oh, S. A. Hong and T. H. Lim, *J. Power Sources*, 2006, **158**, 1246.
32 R. Narducci, M. D. Vona and P. Knauth, *J. Membr. Sci.*, 2014, **465**, 185.
33 S. Gandhimathi, H. Krishnan, D. Paradesi and R. Jeyalakshmi, *Polym. J.*, 2017, **49**, 703.
34 K. Hooshyari, M. Javanbakht, P. Salarizadeh and A. Bageri, *J. Iran. Chem. Soc.*, 2019, **16**, 1617.
35 L. Unnikrishnan, S. K. Nayak, S. Mohanty and G. Sarkhel, *Polym.-Plast. Technol. Eng.*, 2010, **49**, 1419.
36 S. Gandhimathi, H. Krishnan and D. Paradesi, *High Perform. Polym.*, 2020, **32**(3), 296.
37 D. Paradesi, S. Gandhimathi, H. Krishnan, B. Baskar and G. T. Senthil Andavan, *J. Macromol. Sci., Part A: Pure Appl. Chem.*, 2019, **56**(2), 146.
38 W. L. Harrison, F. Wang and J. B. Mecham, *J. Polym. Sci., Part A: Polym. Chem.*, 2003, **41**, 2264.
39 D. Paradesi, S. Gandhimathi, H. Krishnan and R. Jeyalakshmi, *High Perform. Polym.*, 2018, **30**(1), 116.
40 J. F. Blanco, Q. T. Nguyen and P. Schaetzel, *J. Membr. Sci.*, 2001, **186**, 267.
41 H. B. Park, S. Y. Nam, J. W. Rhim, J. M. Lee, S. E. Kim, J. R. Kim and Y. M. Leeet, *J. Appl. Polym. Sci.*, 2002, **86**, 2611.
42 D. Paradesi, D. Samantha, A. B. Mandal and S. N. Jaisankar, *RSC Adv.*, 2014, **4**, 26193.
43 E. E. Abdel-Hady, H. F. M. Mohamed, M. O. Abdel-Hamed and M. M. Gomaa, *Adv. Polym. Technol.*, 2019, **37**, 3842.
44 N. Agmon, *Chem. Phys. Lett.*, 1995, **244**, 456.
45 K. D. Kreuer, *Solid State Ionics*, 1997, **94**, 55.
46 K. D. Kreuer, A. Rabenau and W. Weppner, *Angew. Chem., Int. Ed.*, 1982, **21**, 206.
47 C. L. Robert, K. Valle, F. Pereira and C. Sanchez, *Chem. Soc. Rev.*, 2011, **40**, 961.
48 A. Anis and S. M. Al-Zahrani, *Int. J. Electrochem. Sci.*, 2012, **7**, 9174.
49 S. Khilari, S. Pandit, M. M. Ghangrekar, D. Pradhan and D. Das, *Ind. Eng. Chem. Res.*, 2013, **52**, 11597.
50 Z. Li, X. Zhang, C. Zhou and D. Sun, *Polym. Polym. Compos.*, 2012, **20**(4), 407.
51 R. Vani, S. Ramaprabhu and P. Haridoss, *Sustainable Energy Fuels*, 2020, **4**, 1372.
52 G. M. Aparicio, R. A. Vargas and P. R. Bueno, *J. Non-Cryst. Solids*, 2019, **522**, 119520.
53 S. Meenakshi, S. D. Bhat, A. K. Sahu, S. Alwin, P. Sridhar and S. Pitchumani, *J. Solid State Electrochem.*, 2012, **16**, 1709.